Integrating Image Preprocessing and Pretrained CNN Using Transfer Learning for CRC Diagnosis

Dr. P. Indra, *Assistant Professor, Department of Electronics and Communication Engineering., Government College of Engineering Salem, Tamil Nadu, India*.

N. Muhilarasi, *PG Scholar., Communication Systems, Department of Electronics and Communication Engineering., Government College of Engineering Salem, Tamil Nadu, India.*

Manuscript Received: Apr 08, 2025; Revised: Apr 10, 2025; Published: Apr 18, 2025

Abstract: Colorectal cancer is one of the leading causes of cancer-related mortality worldwide, where early diagnosis for CRC plays a critical role in improving patient outcomes and survival rates. This study presents a hybrid model that integrates traditional image processing techniques with deep learning using pretrained convolutional neural networks (CNNs) to enhance the detection of colorectal cancer from histopathology images. The Preprocessing phase utilizes a progressive switching median filter to enhance image quality by reducing noise without compromising essential histopathological details. Following denoising, the Superpixel SLIC (Simple Linear Iterative Clustering) algorithm performs precise image segmentation, isolating key regions of interest for improved feature extraction. In the classification phase, three convolutional neural network (CNN) architectures—DenseNet, ResNet50, and EfficientNet—are employed to classify colorectal cancer from histopathology images. Each network's performance is evaluated based on accuracy in the classification stage, with DenseNet achieving the highest accuracy of 99.32%, followed by EfficientNet with 98.05%, and ResNet50 with 95.99%. The proposed hybrid model demonstrates that integrating sophisticated image processing with pretrained CNN models enhances diagnostic performance, offering a robust and accurate tool for automated colorectal cancer detection. This hybrid approach could support pathologists in identifying cancerous tissues more effectively, potentially improving patient outcomes.

Keywords: CRC, Histopathology, SLIC, Resnet-50, Densenet-201, Efficientnet-b0

1. Introduction:

According to statistics announced in 2024, colorectal cancer is the second most common type of cancer worldwide, responsible for 10% of new cases and 52,550 deaths each year. Early diagnosis is very important because 25-50% of patients experience recurrence or metastasis. Changes in normal flora led to the development of colon cancer, including the formation of adenomatous polyps. Malignant polyps can spread using lymph and blood vessels, infect nearby tissues, and travel to distant sites. Screening tests include colonoscopy, fecal occult blood test (FOBT), fecal immunochemical test (FIT), CT colonography (virtual colonoscopy), sigmoidoscopy, and fecal DNA test. Late diagnosis is associated with poor outcomes. Histopathological images provide doctors with raw data for diagnosing various cancers. The process of reviewing and analyzing medical images is often complex, time-consuming, and prone to human error. These problems have led to the increasing use of image-based diagnostics, a new research trend today. Computer technology has advanced to the point where histological images can be processed for segmentation, feature extraction, and classification tasks. This paper investigates and evaluates the use of filters in preprocessing of histopathology images and presents improved filters. The best method is selected among various parameters such as MSE, PSNR and SSIM values. Image segmentation is a method used to identify image pixels in the decision-making process. This process divides the image into several separate regions and the pixels in the inhomogeneous regions have similar values in each region and different heights between regions. Superpixel SLIC (Simple Linear Iterative Clustering) algorithm performs accurate image segmentation by introducing high F1 scores, Dice coefficients and IOU and isolates the key regions of interest for advanced feature extraction. In the inference and classification process, three convolutional neural network (CNN) architectures, namely DenseNet-201, ResNet50 and EfficientNet-b0, were used to classify benign and malignant cancer cells from histopathological images. The performance of each network is measured by overall accuracy, overall recall, overall F1 score and model accuracy. The reported hybrid model demonstrates that combining image processing with CNN preprocessing model can improve diagnosis and provide a powerful and accurate tool for diagnosing colorectal cancer.

International Journal of Current Research and Techniques (IJCRT)
E-ISSN: 2349-3194 (Online) | P-ISSN: 2348-4446 (Print)
UGC Approved Journal No: 47722 [No: 2616]
DOI: https://doi.org/10.5281/ZENODO.15239367

2. Related Work

Chun Cheng Peng and Bing Rong Lee (2023) highlighted the potential of CNNs in enhancing the precision and speed of medical diagnostics, particularly for complex medical image classification. Addressing the critical need for early detection of colorectal cancer, they developed a method combining transfer learning with a ResNet50 CNN model optimized using Adam. Their approach achieved exceptional performance, with a training accuracy of 99.02% and a validation accuracy of 99.57%, demonstrating the method's effectiveness in classifying colorectal cancer histopathology images [1].

Mohsan Tanveer and Muhammad Usman Akram (2024) introduced the "TransNetV" model, which combines the local feature extraction strengths of CNNs with the global contextual understanding of Transformers. This hybrid approach utilizes CNNs' weight-sharing properties and Transformers' ability to analyze spatial relationships in complex patterns, ensuring effectiveness on diverse datasets. The model was trained on the NCT Biobank CRC dataset and tested on the CRC-HE-VAL-7K and Kather_texture_2016_5000 datasets, achieving exceptional classification accuracies of 98.54% and 98.96%, respectively. Additionally, the TransNetV architecture is adaptable to other CNN models like ResNet50, ResNet101, and VGG19 [2].

Min Li, Xiaojian Ma, Chen Chen, and Yushuai Yuan (2021) proposed a machine learning-based auxiliary diagnosis model for lung cancer (LC). They extracted multidimensional features from 121 LC histopathological images and employed the Relief algorithm for feature selection. An SVM classifier was then used to classify LC subtypes, with ROC curves and AUC values assessing the classifier's generalization ability. Comparative experiments with other classification models demonstrated that the Relief-SVM model achieved superior performance, with LUSC-ASC classification accuracy of 73.91%, LUSC-SCLC accuracy of 83.91%, and ASC-SCLC accuracy of 73.67%. The results highlight the potential of ML in assisting LC diagnosis [3].

Shahid Mehmood, Taher M. Ghazal, and Muhammad Adnan Khan (2022) developed a highly accurate and efficient model for diagnosing lung and colon cancers. Using 25,000 histopathology images evenly divided into five classes, they fine-tuned AlexNet by modifying four layers. Initial accuracy was 89%, but a simple contrast enhancement applied to the underperforming class boosted accuracy to 98.4% while maintaining computational efficiency [4].

3. Employed Cancer Dataset

All images are RGB, 0.495 µm per pixel, digitized with an Aperio ScanScope (Aperio/Leica biosystems), magnification 20x. Histological samples are fully anonymized images of formalin-fixed paraffin-embedded human colorectal adenocarcinomas (primary tumors) from our pathology archive (Institute of Pathology, University Medical Center Mannheim, Heidelberg University, Mannheim, Germany). There are 5000 histopathology images of benign and malignant type tissues of colorectal cancer, some of shown in the Figure 1.

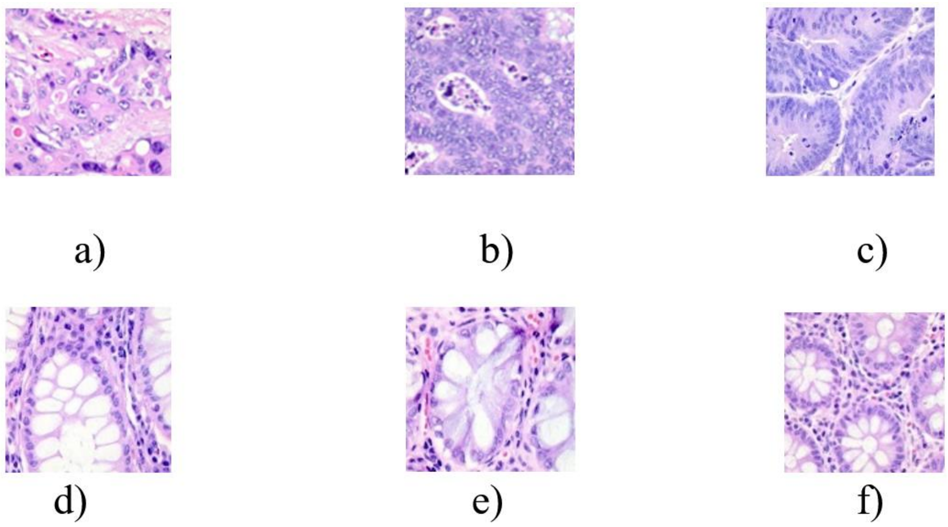

Figure-1 Histopathological images from dataset. Malignant tissues a, b and c. Benign tissues d, e and f.

A. Materials and Methods

Table-1 Materials And Methods

Dataset & Link	Histopathology colon cancer dataset https://zenodo.org/record/53169#.W6HwwP4zbOQ
Number of images	5000
Tools used	MATLAB R2022b

Table I shows the materials and methods used for the proposed work.

4. Proposed Methodology

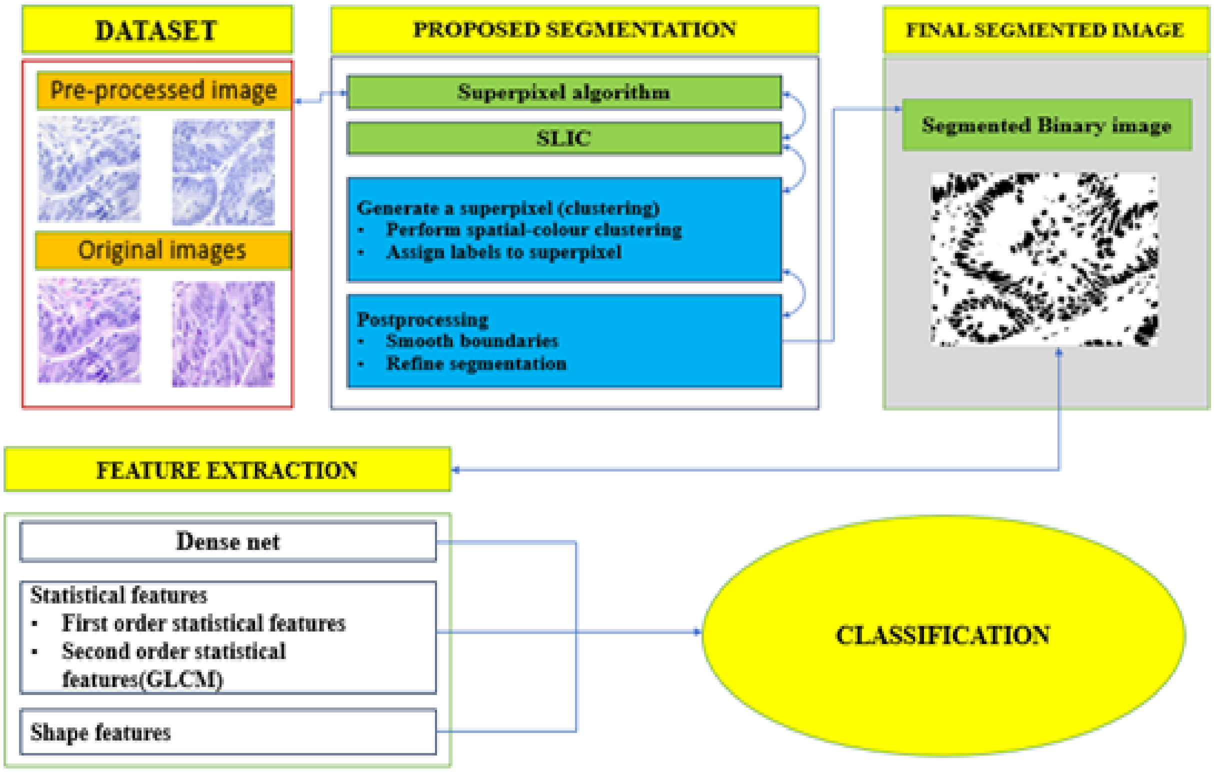

Figure-2 Proposed Methodology for the detection of colorectal cancer

The proposed methodology addresses the presence of noise in histopathology images, such as salt-and-pepper, Gaussian, and speckle noise, by applying various filtering techniques and selecting the optimal filter based on performance metrics. Superpixel segmentation, as illustrated in Figure 2, was identified as the best approach for isolating the region of interest (ROI) due to its superior performance in metrics such as Dice coefficient, F1 score, and Union over Separation (IOU). The segmented images were then used for feature extraction and classification, leveraging pretrained networks including DenseNet-201, EfficientNet-B0, and ResNet-50. These networks were evaluated based on classification accuracy, overall recall, and F1 score, and the most effective model was selected for accurately distinguishing between benign and malignant colorectal cancer types.

The following steps are involved in this proposed work,

A. Image pre-processing

B. Image segmentation

C. feature extraction and

D. Classification based on pretrained neural network

A. Image pre-processing

Medical image denoising plays a crucial role in enhancing diagnostic accuracy and improving the reliability of clinical decisions. It reduces noise and artifacts introduced during image acquisition, thereby preserving essential anatomical and pathological details. Effective denoising not only improves image quality but also ensures better performance of downstream tasks such as segmentation, feature extraction, and classification in Automated driven diagnostic systems.

1) Progressive switching median filtering: A median-based filtering technique, known as the Progressive Switching Median (PSM) filter, is employed to restore images affected by salt-and-pepper impulse noise. This algorithm is designed around two key principles: i) a switching mechanism, where an impulse detection algorithm identifies noisy pixels prior to filtering, ensuring that only a subset of all pixels is processed, and ii) a progressive approach, in which both the detection of impulses and the noise filtering are iteratively refined over multiple passes.

$$O\ (p,q)\ =\ medfilt2\{I\ (p-i,q-j),i,q\} \tag{1}$$

Here, I (p, q) denote the input image, while O (p, q) represents the filtered output image. M specifies the dimensions of the filter mask, with a size of m × m

2) Gaussian filtering techniques: Gaussian filtering is a critical technique used for noise reduction and smoothing in digital images. It involves applying a Gaussian kernel to the image, which assigns more weight to central pixels compared to their surrounding regions. This process effectively reduces noise while preserving the essential structure of the image

$$\mathrm{g}_{\sigma,\mu}(\mathrm{x}) = \frac{1}{\sqrt{2\Pi\sigma}}\exp\left(-\frac{(\mathrm{x}-\mu)^2}{\partial\sigma^2}\right) \tag{2}$$

3) Wiener filtering techniques: Wiener filter is a nonlinear filtering technique utilized for restoring images that are blurred and noisy. It is applied to grayscale images for effective noise reduction and deblurring. The output of the Wiener filter is defined as

$$O\ (p,q)\ = wiener2(I\ (p-i,q-j),nxn) \tag{3}$$

Here, I (p, q) represent the input image, O (p, q) denotes the resulting filtered image, and nxn specifies the dimensions of the image

B. Image segmentation

Image segmentation is essential in medical histopathology, enabling precise analysis of tissue samples by isolating regions of interest-like cells or abnormal structures. It aids in accurate disease diagnosis, quantitative measurements, and treatment planning by highlighting critical features such as tumour boundaries and tissue organization. Automated segmentation enhances efficiency with consistent results, while also serving as a foundation for AI models to improve diagnostic accuracy and predictive capabilities. This makes segmentation indispensable for advancing research, diagnostics, and therapeutic strategies in histopathology.

1) Otsu's threshold segmentation:Otsu's method is used to perform automatic image thresholding to separate the foreground and background in grayscale images. Histogram Analysis: It analyzes the histogram of pixel intensities to find an optimal threshold value that minimizes intra-class variance (variance within the foreground and background). Threshold Selection: The algorithm searches for a threshold value that divides the histogram into two classes, foreground and background, by maximizing the variance between these two classes.

Compute the Grayscale Histogram:

$$H(\mathrm{i}) = \sum_{x=1}^{m}\sum_{y=1}^{n}[I(x,y) = \mathrm{i}] \tag{4}$$

International Journal of Current Research and Techniques (IJCRT)
E-ISSN: 2349-3194 (Online) | P-ISSN: 2348-4446 (Print)
UGC Approved Journal No: 47722 [No: 2616]
DOI: https://doi.org/10.5281/ZENODO.15239367

Compute the Cumulative Distribution Function:

$$c(\mathrm{i}) = \sum_{j=0}^{i} \frac{H(i)}{MxN} \tag{5}$$

Compute the Mean Grayscale Intensity Value of the Image:

$$\mu = \frac{1}{M \times N} \sum_{x=1}^{M} \sum_{y=1}^{N} I(x, y) \tag{6}$$

Find the Threshold Value That Maximizes the Between-Class Variance

$$T_{OPt} = argmax_T(\mathrm{Var}(T)) \tag{7}$$

the below figure 3 shows the Otsu's Threshold segmentation process

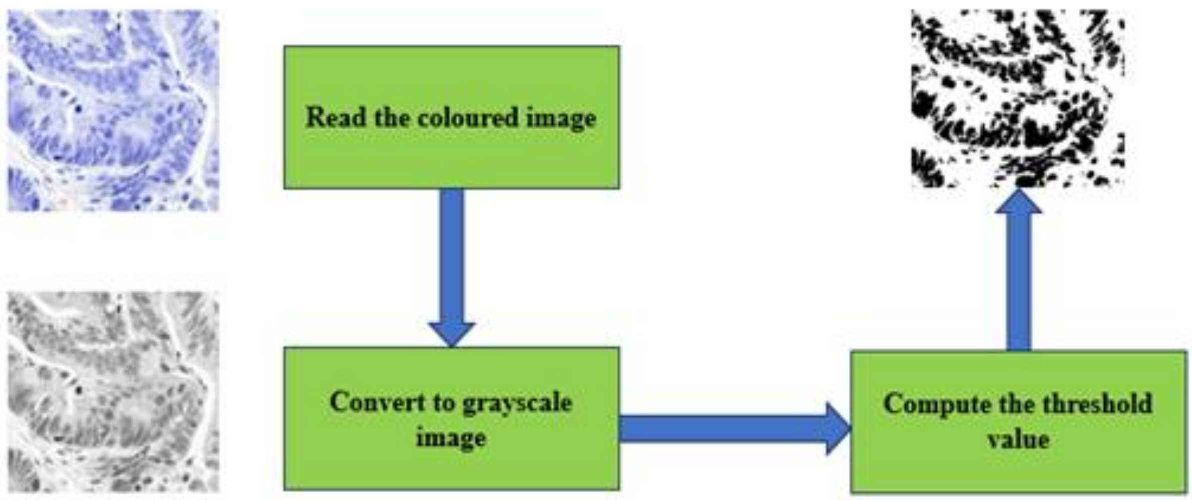

Figure-3 Otsu's threshold techniques

Superpixel oversegmentation: SLIC (Simple Linear Iterative Clustering) algorithm is used to segment an image into superpixel, which are clusters of pixels that have similar color and spatial proximity, resulting in regions that capture meaningful local patterns as shown in figure 4. Cluster Initialization: It initializes cluster centers (seeds) across the image in a regular grid pattern, spacing them approximately equally, based on the desired number of superpixel. Color and Spatial Distance: SLIC calculates a distance measure that combines both color similarity and spatial proximity, forming a weighted Euclidean distance in a five-dimensional space (Lab color space and spatial coordinates).

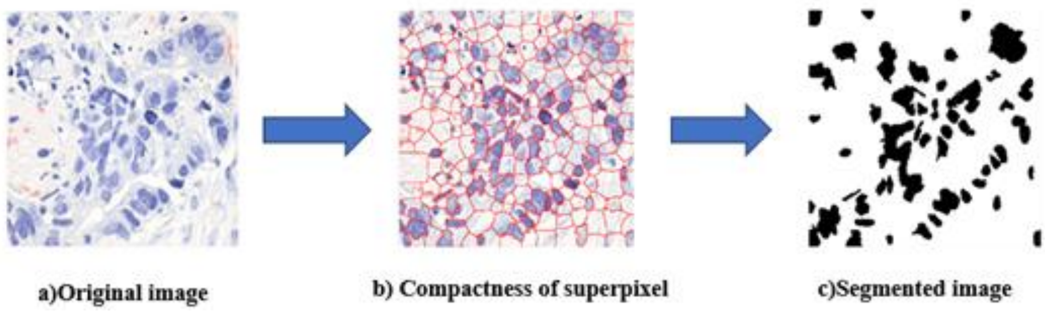

Figure-4 Superpixel segmentation techniques (SLIC)

E-ISSN: 2349-3194 (Online) | P-ISSN: 2348-4446 (Print)
UGC Approved Journal No: 47722 [No: 2616]
DOI: https://doi.org/10.5281/ZENODO.15239367

3) Grey-level threshold segmentation:

Grey level thresholding is used to convert a grayscale image into a binary image by separating objects (foreground) from the background based on pixel intensity. Threshold Value: A threshold value, T, is chosen to divide the grayscale image into two classes: pixels below T (background) and pixels equal to or above T (foreground) which is represented in the below figure 5.

Binary Segmentation: Each pixel intensity I (x, y) is compared to T:

$$\text{Binary}(x, y) = \begin{cases} 1 \text{ if } I(x, y) \geq I \\ 0 \text{ if } I(x, y) < I \end{cases} \tag{8}$$

where 1 represents foreground and 0 represents background in the binary image.

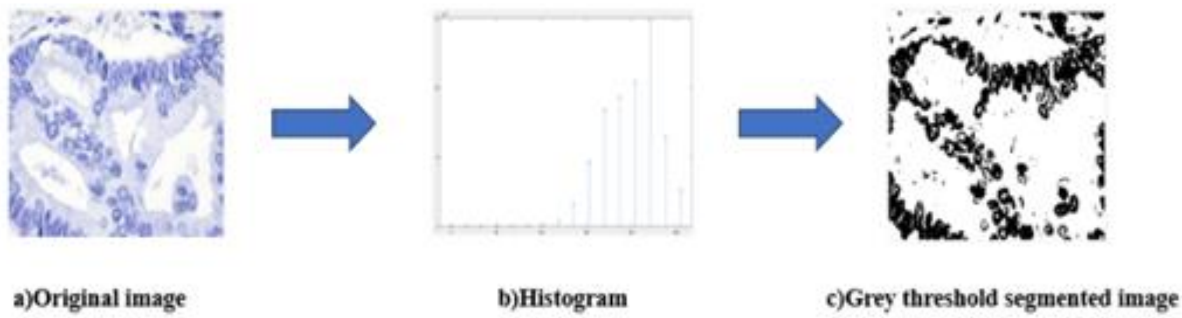

Figure-5 Grey threshold segmentation techniques

C. Feature extraction

Feature extraction using pretrained neural networks is revolutionizing the analysis of medical histopathology images by capturing intricate details like cellular structures and morphological variations. These models eliminate the need for manual feature engineering, offering faster and more accurate identification of pathological patterns. Leveraging their hierarchical learning capabilities, they enhance disease classification, grading, and biomarker discovery. By efficiently processing large datasets, pretrained networks are driving advancements in computational pathology, improving diagnostic accuracy, scalability, and reproducibility.

1) Resnet-50 Architecture: ResNet50, a prominent ResNet architecture, comprises 50 layers and set a benchmark with its state-of-the-art performance on the ImageNet dataset in 2015. It features 16 residual blocks, each made up of multiple convolutional layers interconnected by residual connections.

Input layer accepts 224x224x3 RGB images as input. Convolutional Layers extract features from images using convolutional filters, producing feature maps for further processing. Batch Normalization layer enhances convergence, generalization, and regularization in the network. ReLU Activation function introduces nonlinearity, outputting the input if positive or 0 if negative. Max pooling process reduces spatial dimensions while preserving essential features, lowering computational costs. Flatten layer converts multidimensional outputs into a 1D vector for subsequent layers. Fully connected layers are the final dense layers where neurons are connected to all previous neurons, producing the predictions. Identity block maintains input-output dimensions using three convolutional layers with batch normalization and ReLU activations. Projection block handles input-output dimension mismatches using down sampling and depth adjustments. Global average pooling layer reduces spatial dimensions by averaging feature maps, resulting in a compact feature vector. The layers of Resnet-50 are given below in the figure 6.

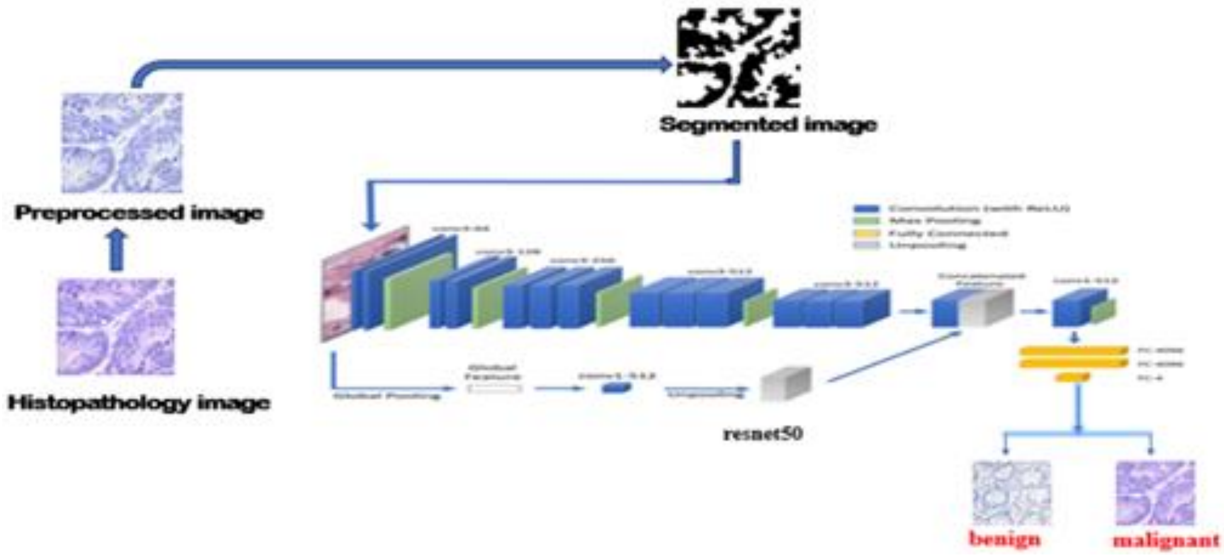

Figure-6 Resnet-50 Architecture

2) Densenet-201 architecture: DenseNet-201 Overview: A 201-layer deep neural network designed to enhance feature reuse and mitigate the vanishing gradient problem through dense connectivity.

Input layer processes a RGB images with a 7×7 convolutional layer, followed by batch normalization and ReLU activation for feature extraction and normalization. Dense blocks consist of layers connected to all previous layers within the block, performing batch normalization, ReLU activation, 1×1 bottleneck convolutions, and 3×3 spatial feature extraction. Each layer in a dense block adds 32 feature maps, promoting efficient feature learning. Transition layers are placed between dense blocks to downsample feature maps using 1×1 convolutions, batch normalization, and 2×2 average pooling.

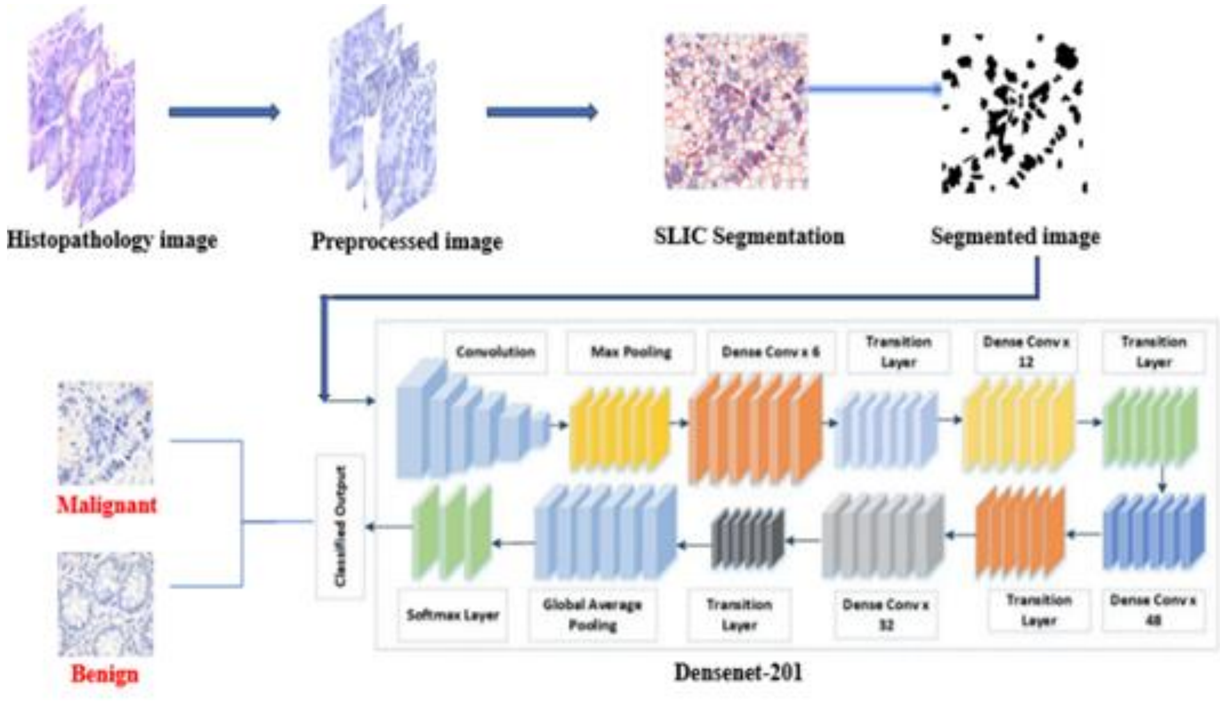

Figure-7 Densenet-201 Architecture

The architecture comprises four dense blocks separated by three transition layers. Global Average Pooling (GAP) layer reduces each feature map to a single value by averaging, minimizing parameters and preventing overfitting. Classification layer: A fully connected layer generates class scores, with SoftMax activation providing probabilities for classification. The layers of densenet-201 architecture are shown in figure 7.

2) Efficientnet-b0 Architecture: EfficientNet-B0 Overview: A high-performance, efficient convolutional neural network that uses compound scaling to optimize network width, depth, and resolution.

Input layer accepts a RGB images, balancing computational efficiency with performance. Stem Block layer which features a 3×3 convolutional layer with 32 filters and stride 2 for low-level feature extraction, followed by batch normalization and Swish activation for improved non-linearity. The bottleneck block used as the basic building block of MobileNetv2 is the MBConv (building block of EfficientNet). MBConv block is the architecture's core, using depthwise separable convolutions and an expansion phase for efficiency. First Group has one MBConv1 block (16 filters, stride 1) for low-level features. Second Group has two MBConv6 blocks (24 filters, stride 2) for complex pattern capture. Third Group has Two MBConv6 blocks (40 filters, stride 2) for mid-level feature extraction. Fourth Group has three MBConv6 blocks (80 filters, stride 2) for high-level features. Fifth Group has three MBConv6 blocks (112 filters, stride 1) for feature refinement. Sixth Group has four MBConv6 blocks (192 filters, stride 2) for intricate pattern learning and Seventh Group has one MBConv6 block (320 filters, stride 1) as a transition to final layers. Global average pooling Layer Condenses each feature map into a single value by averaging spatial dimensions, reducing size while retaining global information. Fully connected layer transforms GAP output into 1280 units for feature refinement before classification. Output Layer has a SoftMax activation function provides class probabilities for the target dataset (e.g., 1000 classes for ImageNet). The step-by-step process of efficientnet-b0 are given below in the figure 8.

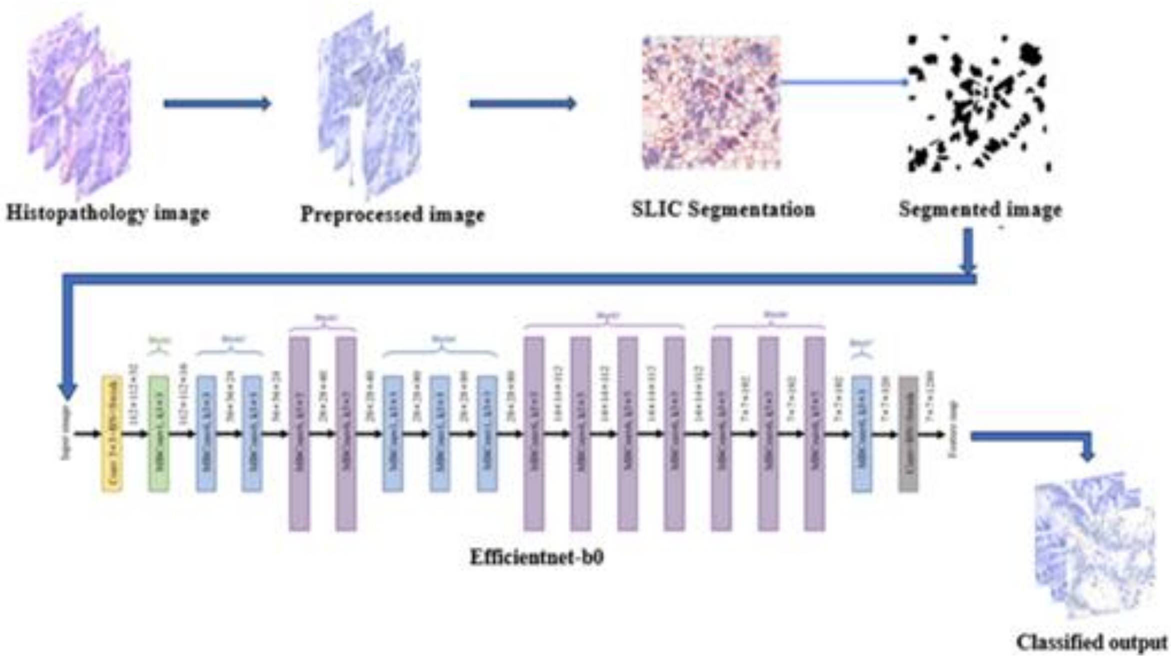

Figure-8 Efficientnet-b0 Architecture

5. Evaluation Results and Discussion

A. Results of filtering techniques:

The proposed filtering methods were applied on different images and some results are given below Figure 9, indicates the original image, output image of three filters. To compare the noise removal techniques, some of performance parameters has been evaluated.

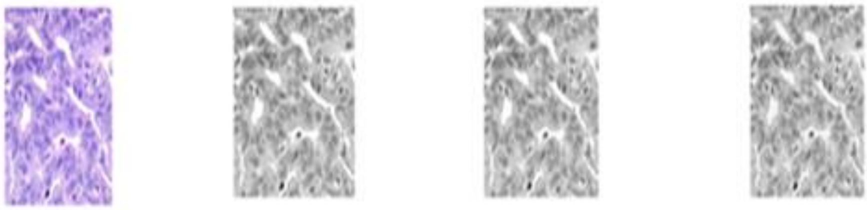

a) Original image 1 filtered by progressive switching median filter, Gaussian filter and wiener filter

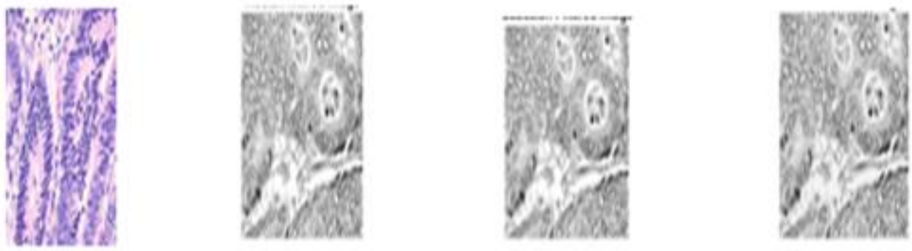

b) Original image 2 filtered by progressive switching median filter, Gaussian filter and wiener filter

Figure-9 Original images and original images filtered by progressive switching median filter, gaussian filter and wiener filter.

The performance of progressive switching median, wiener and gaussian filters are compared by using the quality measures via mean square error (MSE), peak signal-to-noise ratio (PSNR) and structural similarity index measure (SSIM). By this comparison, the best method is selected for further process. Table II shows the comparison of MSE, PSNR and SSIM values of input images

Table-2 Comparison Table Of MSE, PSNR And SSIM Values For Some Images

Parameters	Preprocessed image / Filters	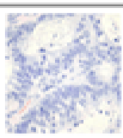	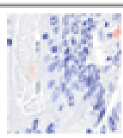	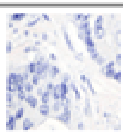	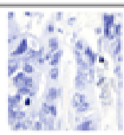	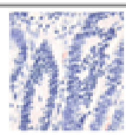
MSE	Wiener filter	386.7385	392.2611	368.2858	411.1434	400.2229
	Gaussian filter	20.9423	31.8434	61.7409	29.6761	71.7995
	Progressive switching median filter	2.3537	3.5821	5.3902	3.3221	10.9169
PSNR	Wiener filter	22.2566	22.1951	22.4690	21.9909	22.1078
	Gaussian filter	34.9206	33.1006	30.2251	33.4067	29.5696
	Progressive switching median filter	44.4133	42.5894	40.8147	42.9167	37.7498
SSIM	Wiener filter	0.5028	0.5156	0.5698	0.5078	0.5292
	Gaussian filter	0.9240	0.8961	0.8742	0.8895	0.7495
	Progressive switching median filter	0.9875	0.9827	0.9849	0.9832	0.9605

B. Results of Segmentation Methods.

The proposed segmentation methods were applied on different histopathological images and the results are given below in Figure 10, which shows the results of segmentation which includes superpixel (SLIC) algorithm, Otsu's

E-ISSN: 2349-3194 (Online) | P-ISSN: 2348-4446 (Print)
UGC Approved Journal No: 47722 [No: 2616]
DOI: https://doi.org/10.5281/ZENODO.15239367

threshold segmentation and grey threshold segmentation after image binarization method for benign and malignant cases.

Figure-10 filtered image, Otsu's segmented, superpixel segmented and grey threshold segmented images of malignant cases.

Table-3 Comparison Table Of Segmentation Methods For Some Image

Parameters	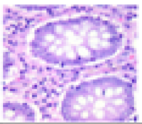			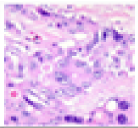			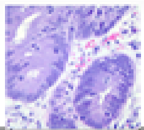		
	Otsu's threshold	Superpixel segmentation	Gray threshold	Otsu's threshold	Superpixel segmentation	Gray threshold	Otsu's threshold	Superpixel segmentation	Gray threshold
Dice Coefficient	0.8414	0.8505	0.7542	0.7721	0.7865	0.5124	0.8614	0.9017	0.7711
F1 Score	0.8414	0.8505	0.7542	0.7721	0.7865	0.5124	0.8614	0.9017	0.7711
Accuracy	0.8233	0.8331	0.3485	0.8872	0.8946	0.3025	0.8453	0.9246	0.5012
Recall	0.6058	0.5531	0.5081	0.5152	0.5764	0.4413	0.2573	0.4514	0.5725
Precision	0.7089	0.6464	0.8087	0.6792	0.5638	0.3024	0.6503	0.6448	0.5012
IOU	0.5582	0.5693	0.5487	0.5446	0.5986	0.3028	0.5479	0.5896	0.5112

The performance of the Superpixel (SLIC) algorithm, Otsu's threshold segmentation, and gray threshold segmentation is compared using quality measures such as Dice coefficient, F1 score, and IOU which represents in the figure 11. Based on this comparison, the best method is selected for further processing. Table 5.2 presents the comparison of Dice coefficient, F1 score, accuracy, recall, precision, and IOU values for the segmented images. Among these three segmentation techniques, the Superpixel segmentation technique (SLIC algorithm) achieves better results with higher Dice coefficient range from (0 to 1), F1 score, and IOU values

E-ISSN: 2349-3194 (Online) | P-ISSN: 2348-4446 (Print)
UGC Approved Journal No: 47722 [No: 2616]
DOI: https://doi.org/10.5281/ZENODO.15239367

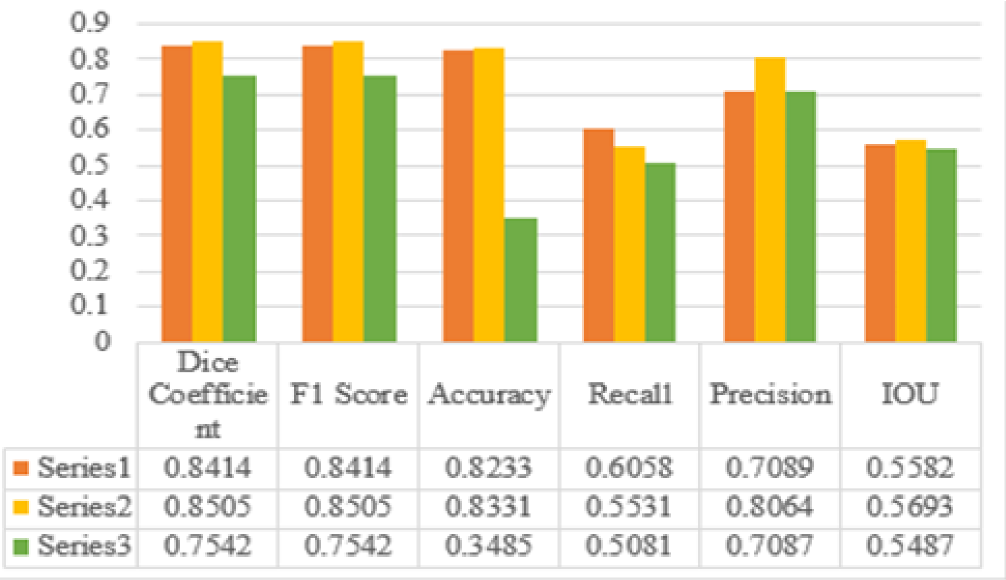

Figure-11. Performance analysis chart of segmentation techniques for some images

C. Results of Feature extraction and classification using pretrained network

Following the segmentation process, superpixel segmented image is given as Input for the feature extraction and classification phase. In this proposed work, three convolutional neural network (CNN) architectures—DenseNet-201, ResNet50, and EfficientNet-b0 are used to classify colorectal cancer from histopathology images. The performance of includes Resnet50, Densenet-201 and Efficientnet-b0 are compared by using the quality measures via Overall Precision, Overall Recall, Overall F1 Score and Classification accuracy.

Performance metrics:

Overall precision:

$$\text{Precision} = \frac{TP}{TP+FP} \tag{9}$$

Overall Recall:

$$\text{Recall} = \frac{TP}{TP+FN} \tag{10}$$

Overall F1 score:

$$\text{F1 Score} = \frac{2TP}{2TP+FP+FN} \tag{11}$$

Classification Accuracy

$$\text{Accuracy} = \frac{\text{Number of correct predictions}}{\text{Total number of predictions}} \tag{12}$$

Table-4 Comparison Table Of Pretrained Neural Networks

International Journal of Current Research and Techniques (IJCRT)
E-ISSN: 2349-3194 (Online) | P-ISSN: 2348-4446 (Print)
UGC Approved Journal No: 47722 [No: 2616]
DOI: https://doi.org/10.5281/ZENODO.15239367

PARAMETERS	PRETARINED NEURAL NETWORKS	VALUES
Overall precision	Efficientnet-b0	97.875%
	Densenet-201	99.290%
	Resnet-50	97.261%
Overall recall	Efficientnet-b0	97.654%
	Densenet-201	99.285%
	Resnet-50	97.104%
Overall F1-score	Efficientnet-b0	97.778%
	Densenet-201	99.285%
	Resnet-50	97.107%
Classification accuracy	Efficientnet-b0	97.826%
	Densenet-201	99.288%
	Resnet-50	97.101%

Table IV shows that the densenet-201 gives the highest score of Overall Precision, Overall Recall, Overall F1 Score and Classification accuracy. so, the densenet-201 is used for diagnosis result to classify whether the colorectal cancer tissue is benign or malignant class.

Figure 12, shows DenseNet achieved the highest classification accuracy of 99.288%, followed by EfficientNet at 97.826%, and ResNet50 at 97.101%. The hybrid approach combining image processing and CNNs significantly improved colorectal cancer detection. DenseNet performed best due to its ability to capture complex patterns in histopathology images.

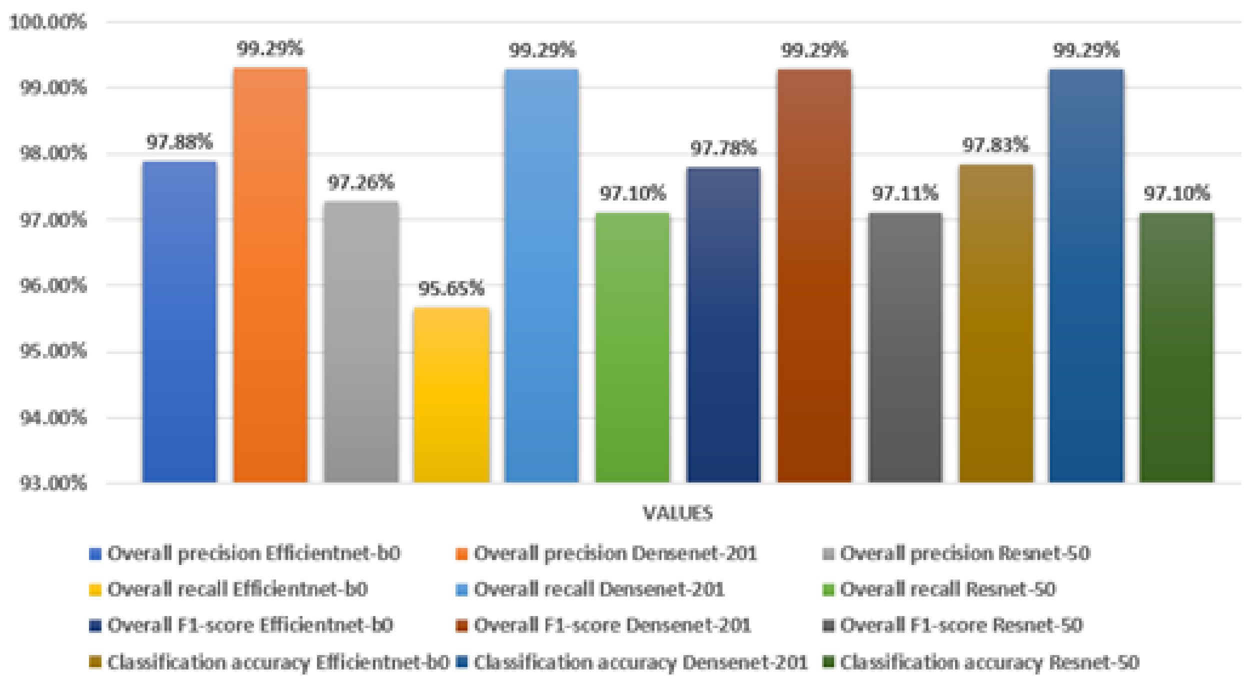

Figure-12 Performance analysis chart of pretrained neural network

Table-5 Confusion Matrix

	Predicted Benign	**Predicted Malignant**
Actual Benign	True Negative (TN)	False Positive (FP)
Actual Malignant	False Negative (FN)	True Positive (TP)

True Positives (TP): Correctly classified malignant cases.

True Negatives (TN): Correctly classified benign cases.

False Positives (FP): Benign cases misclassified as malignant (also called Type I error).

False Negatives (FN): Malignant cases misclassified as benign (Type II error).

Figure 13, 14 and 15 shows the confusion matrix of proposed work using pretrained neural network classifier for classification.

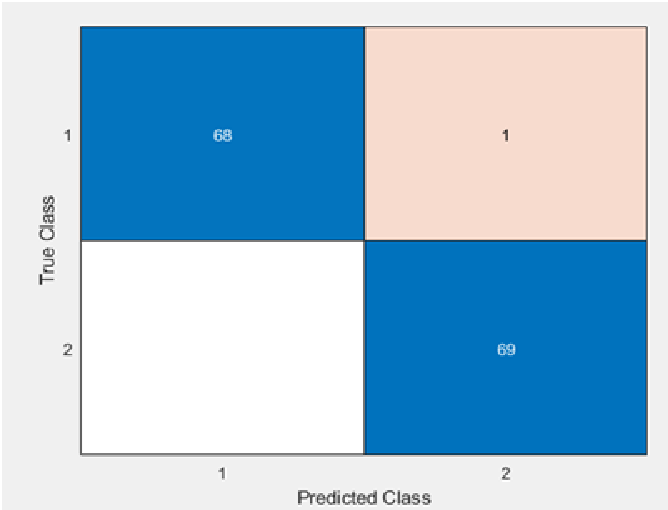

Figure-13 Confusion Matrix of Densenet-201

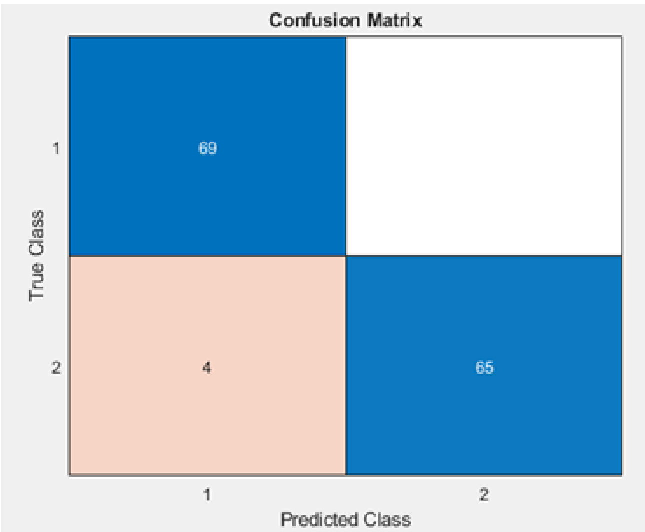

Figure-14 Confusion Matrix of Resnet-50

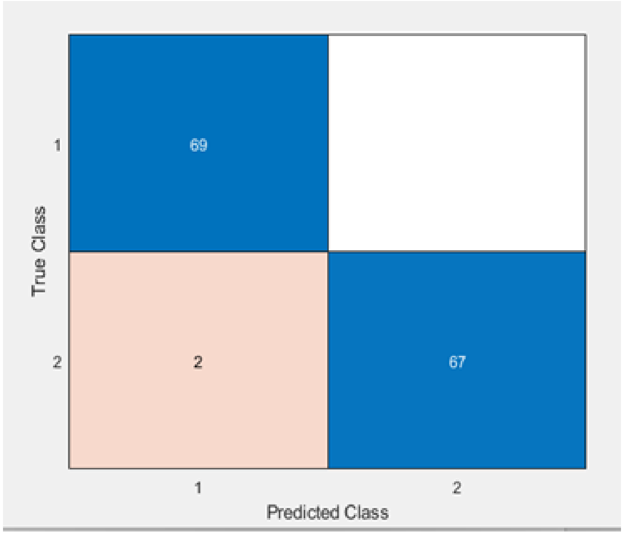

Figure-15 Confusion Matrix of Efficientnet-b0

D. Simulation Results

1) Training Progress of Pretrained Neural Networks

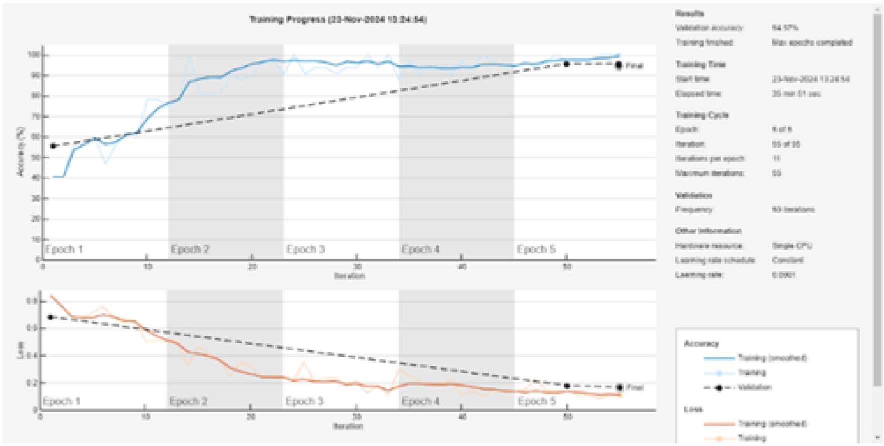

Figure-16 Training progress of proposed work using EfficientNet- b0 classifier

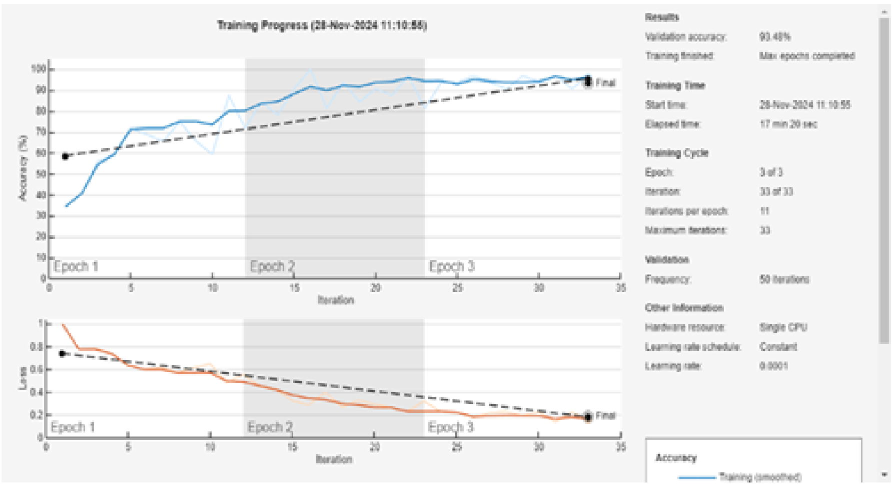

Figure-17 Training progress of proposed work using ResNet- 50 classifier

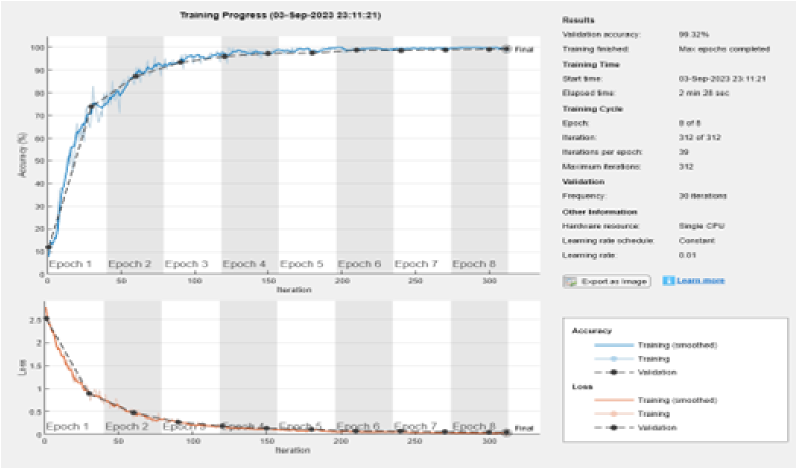

Figure-18 Training progress of proposed work using Densenet-201 classifier

For classification, Densenet-201, Resnet-50, and EfficientNet-b0 were used. Figures 16, 17, and 18 show the training progress of the proposed work using a pretrained neural network classifier for classification. By training progress, it is clearly understood that the validation accuracy of the Densenet-201 architecture achieves 99.32%, followed by EfficientNet-B0 at about 94.57% and ResNet-50 at about 93.48%, so that for the next process, the Densenet-201 network architecture is used to classify the colorectal cancer stages, such as benign and malignant cases.

2) Classification Results

The displayed image represents a binary histopathological sample that has undergone a classification phase using the DenseNet201 deep learning model. This model, known for its efficiency and accuracy in image-based classification tasks, was employed to categorize the image as benign or malignant. Based on the results shown in the pop-up dialogue, the DenseNet201 model successfully classified the image as "benign" and “malignant”. This indicates that the preprocessing steps and model architecture worked effectively, ensuring accurate predictions for benign and malignant cases during the evaluation process.

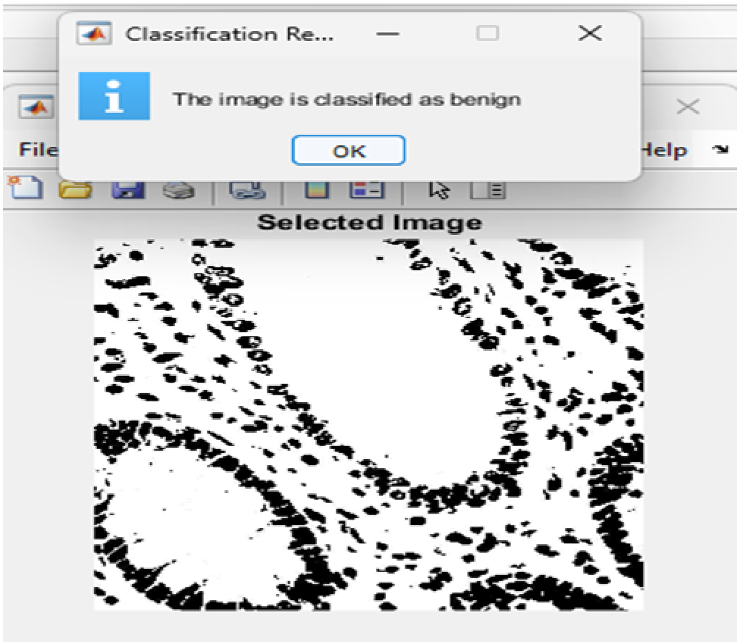

Figure-19 Image is classified as benign tissue

International Journal of Current Research and Techniques (IJCRT)
E-ISSN: 2349-3194 (Online) | P-ISSN: 2348-4446 (Print)
UGC Approved Journal No: 47722 [No: 2616]
DOI: https://doi.org/10.5281/ZENODO.15239367

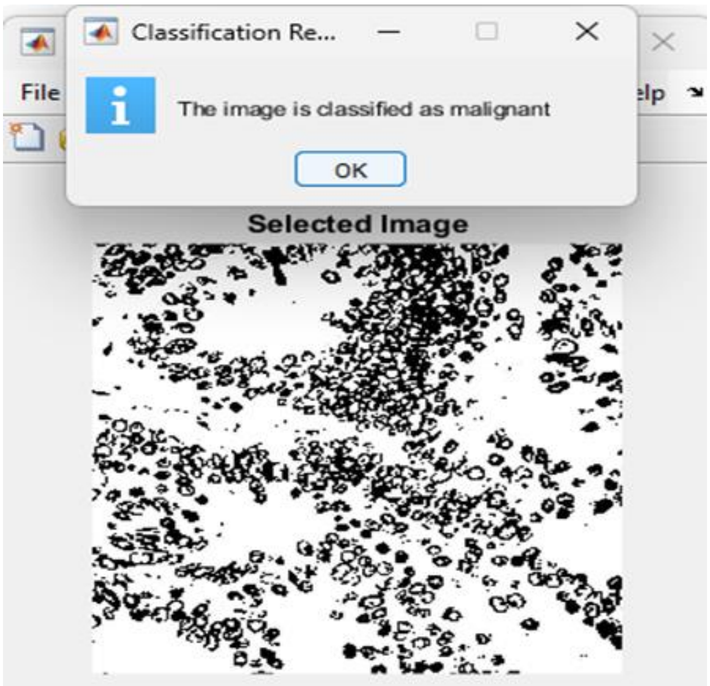

Figure-20 Image is classified as Malignant tissue

Figures 19 and 20 show the classification of the colorectal cancer stage as benign or malignant using the histopathology images by the pre-trained neural network dense net-201 architecture.

6. Conclusion and Future Work

The preprocessing phase utilized a progressive Switching median filter because the filter achieves the low MSE, high PSNR and SSIM value. Superpixel SLIC segmentation to isolate key regions of interest, achieving a high Dice coefficient, F1 score, and Intersection over Union (IOU), which contributed to significantly improved model performance. In the feature extraction and classification phase, three convolutional neural network (CNN) architectures—DenseNet-201, ResNet50, and EfficientNet-b0 are employed to classify colorectal cancer from histopathology images. Each network's performance is evaluated based on Overall Precision, Overall Recall, Overall F1 Score and Classification accuracy. DenseNet achieved the highest classification accuracy of 99.32%, followed by EfficientNet at 97.82%, and ResNet50 at 97.10%. This work proposed a hybrid approach by combining image processing and CNNs significantly for improved colorectal cancer detection. DenseNet performed best due to its ability to capture complex patterns in histopathology images. This model offers a reliable tool to assist pathologists, reducing workload and ensuring consistent cancer diagnosis.

In future aspect,

i. A real-time system can be implemented.

ii. To apply other neural network types

7.References:

[1] Chun Cheng Peng, Bing Rong Lee(2023) "Enhancing Colorectal Cancer Histological Image Classification Using Transfer Learning and ResNet50 CNN Model" Biomedical Signal Processing and Control Volume 96, Part A, October 2024, 106579

[2] D. Sarwinda, R.H. Paradisa, A. Bustamam, and P. Anggia, "Deep learning in image classification using residual network (ResNet) variants for detection of colorectal cancer", Procedia Comput. Sci., vol. 179, pp. 423-431, 2021.

[3] Dmitrii Bychkov, "Deep learning based tissue analysis predicts outcome in colorectal cancer", Scientific Reports , vol. 8, no. 1, p.3395, 2018.

[4] Dr. P. Indra, (2015), "Survey on Mammogram Image Classification CAD system" in the proceedings of Global Journal of Engineering and Applied Sciences (GJEAS) Vol 4, Issue 3, pages:54-56.

[5] Dr. P. Indra, R.Yoganapriya, "Pre-Processing Techniques For Breast Cancer Detection In Mammography Images", International Journal of Novel Research and Development (IJNRD), ISSN: 2456-4184, pp: a79-a83, Volume 8, Issue 7 July 2023.

[6] E. Morgan, M. Arnold, A. Gini, V. Lorenzoni, C. Cabasag, M. Laversanne, J. Vignat, J. Ferlay, N. Murphy, F. Bray, Global burden of colorectal cancer in 2020 and 2040: Incidence and mortality estimates from GLOBOCAN, Gut 72 (2) (2023) 338–344.

[7] E.F. Ohata, J.V.S. Chagas, G.M. Bezerra, M.M. Hassan, V.H.C. de[24] Albuquerque, and P.P.R. Filho, "A novel transfer learning approach for the classification of histological images of colorectal cancer", J. Supercomput., vol. 77, no. 9, pp. 9494-9519, 2021.[http://dx.doi.org/10.1007/s11227-020-03575-6]

[8] J.N. Kather, F.G. Zöllner, F. Bianconi, S.M. Melchers, L.R. Schad, T. Gaiser, A. Marx, C.-A. Weis, Collection of textures in colorectal cancer histology, 2016. [5] M. Veta, P.J.v. Diest, R. Kornegoor, A. Huisman, M.A. Viergever, J.P.W. Pluim, Automatic nuclei segmentation in H&E stained breast cancer histopathology images, PLoS One 8 (7) (2013) e70221.

[9] L. An, L. Wang, Y. Li, HEA-Net: Attention and MLP hybrid encoder architecture for medical image segmentation, Sensors 22 (18) (2022) 7024.

[10] Lin Xu, "Colorectal cancer detection based on deep learning", J.[8] Pathol. Inform., vol. 11, no. 1, p. 28, 2020.[http://dx.doi.org/10.4103/jpi.jpi_68_19]

[11] M. Aloraini, A. Khan, S. Aladhadh, S. Habib, M.F. Alsharekh, M. Islam, Combining the transformer and convolution for effective brain tumor classification using MRI images, Appl. Sci. 13 (6) (2023) 3680.

[12] M. Rasool, N.A. Ismail, W. Boulila, A. Ammar, H. Samma, W.M. Yafooz, A.-H.M. Emara, A hybrid deep learning model for brain tumor classification, Entropy 24 (6) (2022) 799.

[13] Min Li, Xiaojian Ma, Chen Chen, Yushuai Yuan, Shuailei Zhang (2021) "Research on the Auxiliary Classification and Diagnosis of Lung Cancer Subtypes Based on Histopathological Images" IEEE Access (Volume: 9) DOI: 10.1109/ACCESS.2021.3071057

[14] Min-Jen Tsai, and Yu-Han Tao, "Deep learning techniques for the classification of colorectal cancer tissue", Electronics , vol. 10, no. 14, p. 1662, 2021.

[15] P. Bankhead, M.B. Loughrey, J.A. Fernandez, Y. Dombrowski, D.G. McArt, P.D. Dunne, et al., QuPath: Open source software for digital pathology image analysis, Sci. Rep. 7 (1) (2017) 16878.

[16] P. J. Sudharshan, C. Petitjean, F. Spanhol, L. E. Oliveira, L. Heutte and P. Honeine, "Multiple instance learning for histopathological breast cancer image classification", Expert Syst. Appl., vol. 117, pp. 103-111, Mar. 2019.

[17] Panyun Zhou, "HCCANet: Histopathological image grading of colorectal cancer using CNN based on multichannel fusion attention mechanism", Sci. Rep. , vol. 12, no. 1, p. 15103, 2022. [http://dx.doi.org/10.1038/s41598-022-18879-1]

[18] Q.-D. Pham, H. Nguyen-Truong, N.N. Phuong, K.N. Nguyen, C.D. Nguyen, T. Bui, S.Q. Truong, Segtransvae: Hybrid CNN-transformer with regularization for medical image segmentation, in: 2022 IEEE 19th International Symposium on Biomedical Imaging, ISBI, 2022, pp. 1–5.

[19] R. Cui, R. Yang, F. Liu, C. Cai, N-Net: Lesion region segmentations using the generalized hybrid dilated convolutions for polyps in colonoscopy images, Front. Bioeng. Biotechnol. 10 (2022) 96359.